

**Table S1. Table of strains used in this study.**

Strain	Genotype	Source or reference
<b>Figure 1</b>		
AP240	<i>ade6-M210 ura4-D18 leu1-32 h-</i>	Laboratory collection
AP5400	<i>AP240 + pAF12 (pREP3X-Erg25) ade6-M210 ura4-D18 leu1-32</i>	This study
<b>Figure 2</b>		
AP5507	<i>cdr2-EGFP:kanMX6, rlc1-mcherry:natMX6, sid4-mcherry:hphMX6 ade6-M210 ura4-D18 leu1-32</i>	This study
AP5511	<i>cdr2-EGFP:kanMX6, rlc1-mcherry:natMX6, sid4-mcherry:hphMX6 + pAF12 (pREP3X-Erg25) ade6-M210 ura4-D18 leu1-32</i>	This study
AP5718	<i>blt1-mEGFP:kanMX6, rlc1-mcherry:natMX6, sid4-mcherry:hphMX6 ade6-M210 ura4-D18 leu1-32</i>	This study
AP5741	<i>blt1-mEGFP:kanMX6, rlc1-mcherry:natMX6, sid4-mcherry:hphMX6 + pAF12 (pREP3X-Erg25) ade6-M210 ura4-D18 leu1-32</i>	This study
<b>Figure 3</b>		
AP5802	<i>Pact1-lifect-GFP:leu1+, rlc1-mcherry:Nat, sid4-mcherry:hphMX6 ade6-M210 ura4-D18 leu1-32</i>	Laboratory collection
AP5806	<i>Pact1-lifect-GFP:leu1+, rlc1-mcherry:natMX6, sid4-mcherry:hphMX6 + pAF23 (pREP42X-Erg25) ade6-M210 ura4-D18 leu1-32</i>	This study
<b>Figure 4 and Figure S5</b>		
AP5595	<i>mid1-mEGFP:kanMX6, rlc1-mcherry:natMX6, sid4-mcherry:hphMX6 ade6- ura4-D18 leu1-32</i>	This study
AP5621	<i>mid1-mEGFP:kanMX6, rlc1-mcherry:natMX6, sid4-mcherry:hphMX6 + pAF12 (pREP3X-Erg25) ade6- ura4-D18 leu1-32</i>	This study
AP5629	<i>2mYFP-rng2:ura4+, rlc1-mcherry:natMX6, sid4-mcherry:hphMX6 ade6- ura4-D18 leu1-32</i>	This study
AP5665	<i>2mYFP-rng2:ura4+, rlc1-mcherry:natMX6, sid4-mcherry:hphMX6 + pAF12 (pREP3X-Erg25) ade6- ura4-D18 leu1-32</i>	This study

AP5598	<i>GFP-cdc15:kanMX6, rlc1-mcherry:natMX6, sid4-mcherry:hphMX6 ade6- ura4-D18 leu1-32</i>	This study
AP5640	<i>GFP-cdc15:kanMX6, rlc1-mcherry:natMX6, sid4-mcherry:hphMX6 + pAF12 (pREP3X- Erg25) ade6- ura4-D18 leu1-32</i>	This study
<b>Figure 5</b>		
AP5601	<i>cdc12-3YFP:kanMX6, rlc1-mcherry:natMX6, sid4-mcherry:hphMX6 ade6-M210 ura4-D18 leu1-32</i>	This study
AP5635	<i>cdc12-3YFP:kanMX6, rlc1-mcherry:natMX6, sid4-mcherry:hphMX6 + pAF12 (pREP3X- Erg25) ade6-M210 ura4-D18 leu1-32</i>	This study
AP6183	<i>cdc12-3XGFP:kanMX6, rlc1-mcherry:kanMX6, sid4-mcherry:hphMX6 ade6-M210 ura4-D18 leu1-32</i>	From Bohnert et al., 2013 (KG15568)
AP6193	<i>cdc12-3XGFP:kanMX6, rlc1-mcherry:kanMX6, sid4-mcherry:hphMX6 + pAF12 (pREP3X- Erg25)ade6-M210 ura4-D18 leu1-32</i>	This study
AP6129	<i>cdc12-3YFP:kanMX6, rlc1-mcherry:natMX6, sid4-mcherry:hphMX6 cdc25-22 ade6-M210 ura4-D18 leu1-32</i>	This study
AP6145	<i>cdc12-3YFP:kanMX6, rlc1-mcherry:natMX6, sid4-mcherry:hphMX6 cdc25-22 + pAF12 (pREP3X- Erg25) ade6-M210 ura4-D18 leu1-32</i>	This study
AP6166	<i>cdc12-3YFP:kanMX6, rlc1-mcherry:natMX6, sid4-mcherry:hphMX6 cdc25-22 mid1::ura4<sup>+</sup> ade6-M210 ura4-D18 leu1-32</i>	This study
<b>Figure 6</b>		
AP5802	<i>Pact1-lifeact-GFP:leu1+, rlc1-mcherry:natMX6, sid4-mcherry:hphMX6 ade6-M210 ura4-D18 leu1-32</i>	Laboratory collection
AP5806	<i>Pact1-lifeact-GFP:leu1+, rlc1-mcherry:natMX6, sid4-mcherry:hphMX6 + pAF23 (pREP42X- Erg25) ade6-M210 ura4-D18 leu1-32</i>	This study
AP240	<i>ade6-M210 ura4-D18 leu1-32 h-</i>	Laboratory collection
AP5400	<i>AP240 + pAF12 (pREP3X- Erg25) ade6-M210 ura4-D18 leu1-32</i>	This study
TP1032	<i>myo1::kanMX6 h- ade6-M210 leu1-32</i>	from Riken Institute (FY13570)
AP5894	<i>myo1::kanMX6 + pAF12 (pREP3X-Erg25) ade6-M210 leu1-32</i>	This study
<b>Figure S1</b>		

AP240	<i>ade6-M210 ura4-D18 leu1-32 h-</i>	Laboratory collection
AP5400	<i>AP240 + pAF12 (pREP3X-Erg25) ade6-M210 ura4-D18 leu1-32</i>	This study
AP5323	<i>erg6Δ::kanMX6 ade6-M210 ura4-D18 leu1-32</i>	This study
AP5724	<i>erg6Δ::kanMX6 + pAF12 (pREP3X-Erg25) ade6-M210 ura4-D18 leu1-32</i>	This study
AP5716	<i>erg25-ENVY::kanMX6 ade6-M210 ura4-D18 leu1-32</i>	This study
AP5770	<i>erg25-ENVY::kanMX6, (SPAC1B2.03c)ER-marker-mcherry::natMX6 ade6-M210 ura4-D18 leu1-32</i>	This study
AP5790	<i>erg25-ENVY::kanMX6, rlc1-mcherry::natMX6, sid4-mcherry::hphMX6 + pAF12 (pREP3X-Erg25) ade6-M210 ura4-D18 leu1-32</i>	This study
AP5808	<i>scs2Δ::kanMX6 ade6-M210 ura4-D18 leu1-32</i>	This study
AP5843	<i>scs2Δ::kanMX6 + pAF12 (pREP3X-Erg25) ade6-M210 ura4-D18 leu1-32</i>	This study
AP5785	<i>scs22Δ::kanMX6 ade6-M210 ura4-D18 leu1-32</i>	This study
AP5793	<i>scs22Δ::kanMX6 + pAF12 (pREP3X-Erg25) ade6-M210 ura4-D18 leu1-32</i>	This study
AP5837	<i>scs22Δ::kanMX6, scs2Δ::natMX6 ade6-M210 ura4-D18 leu1-32</i>	This study
AP5847	<i>scs22Δ::kanMx6, scs2Δ::natMX6 + pAF12 (pREP3X-Erg25) ade6-M210 ura4-D18 leu1-32</i>	This study
<b>Figure S2</b>		
AP5507	<i>cdr2-EGFP::kanMX6, rlc1-mcherry::natMX6, sid4-mcherry::hphMX6 ade6-M210 ura4-D18 leu1-32</i>	This study
AP5511	<i>cdr2-EGFP::kanMX6, rlc1-mcherry::natMX6, sid4-mcherry::hphMX6 + pAF12 (pREP3X-Erg25) ade6-M210 ura4-D18 leu1-32</i>	This study
AP3788	<i>cdr2-tagRFP::natMX6 mid1-mEGFP::kanMX6 ade6-M210 ura4-D18 leu1-32</i>	Laboratory collection
AP6094	<i>cdr2-tagRFP::natMX6 mid1-mEGFP::kanMX6 + pAF12 (pREP3X-Erg25) ade6-M210 ura4-D18 leu1-32</i>	This study
<b>Figure S3</b>		
AP6184	<i>sid4-GFP::kanMX6, rlc1-mcherry::NatMX6 ade6-M210 ura4-D18 leu1-32</i>	This study
AP6155	<i>sid4-GFP::kanMX6, rlc1-mcherry::NatMX6 + pAF12 (pREP3X-Erg25) ade6-M210 ura4-D18 leu1-32</i>	This study
<b>Figure S4 and S6</b>		

AP5802	<i>Pact1-lifeact-GFP:leu1+, rlc1-mcherry:natMX6, sid4-mcherry:hphMX6 ade6-M210 ura4-D18 leu1-32</i>	Laboratory collection
AP5806	<i>Pact1-lifeact-GFP:leu1+, rlc1-mcherry:natMX6, sid4-mcherry:hphMX6 + pAF23 (pREP42X- Erg25) ade6-M210 ura4-D18 leu1-32</i>	This study

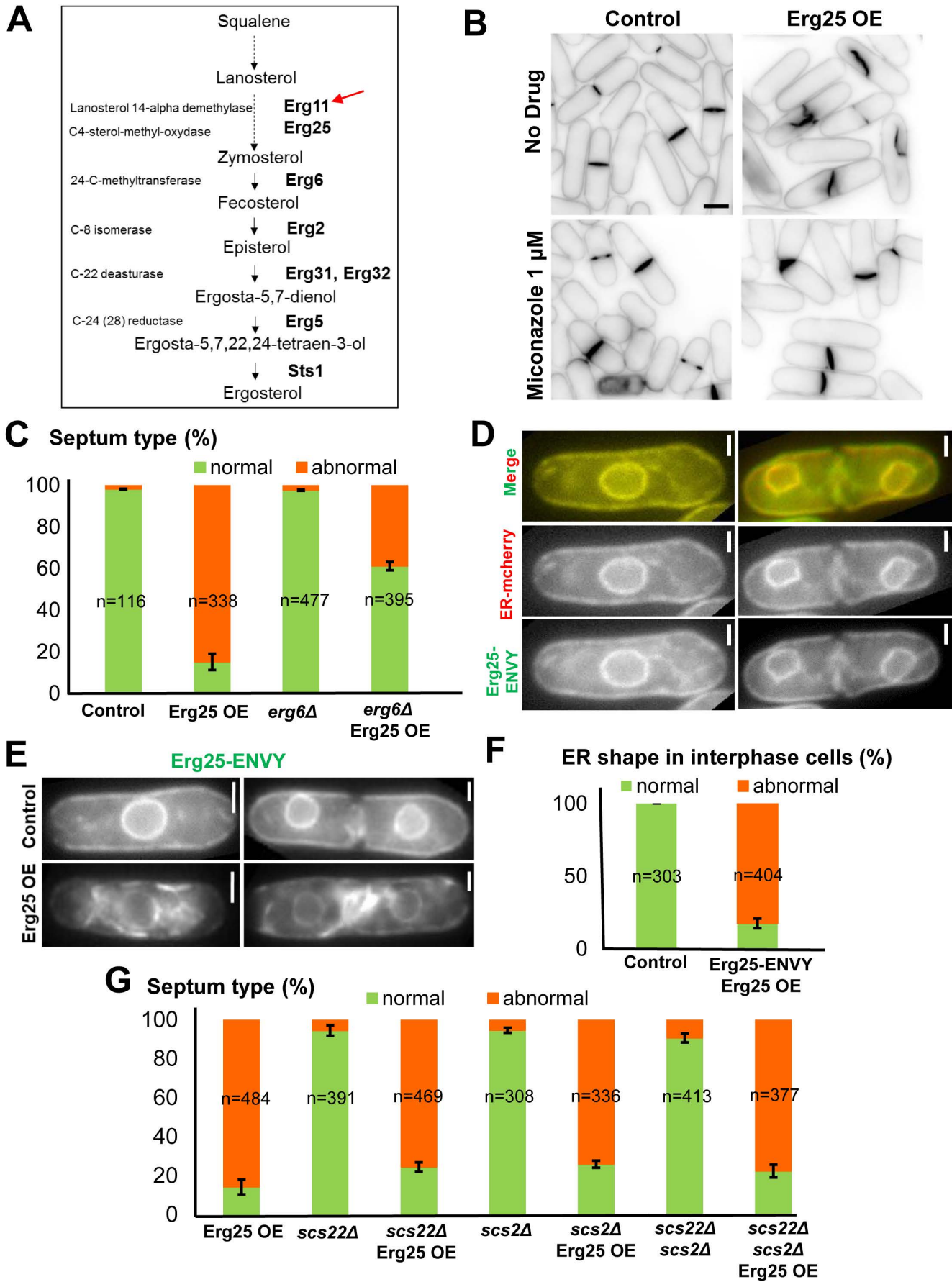


**Figure S1. Cytokinetic defects induced by Erg25 OE require an active sterol biosynthetic pathway, while Erg25 affects ER organization with little impact on division plane positioning.**

**A:** Schematic representation of the late stages of ergosterol biosynthetic pathway in *S. pombe* deduced from *S. cerevisiae* (adapted from Iwaki et al., 2008). The red arrow indicates at which level of the pathway miconazole acts. **B:** Calcofluor staining of control and Erg25 OE cells, treated and non-treated with 1 $\mu$ M miconazole. Scale bar, 5 $\mu$ m. **C:** Quantification of septum defects observed by calcofluor staining of control (n=116), Erg25 OE (n=338), *erg6* $\Delta$  (n=477) and Erg25 OE *erg6* $\Delta$  cells (n=395). Error bars: SD. **D:** Epifluorescence images of Erg25-ENVY and of the ER marker Elo2 fused to mcherry (ER-mcherry). Scale bars: 5 $\mu$ m. **E:** Epifluorescence images of Erg25-ENVY in control (top) and Erg25 OE cells (bottom) in interphase (left) and in late cytokinesis (right). Scale bars: 5 $\mu$ m. **F:** Quantification of ER shape in interphase in control (n=303) and Erg25 OE cells (n=404). Error bars: SD. **G:** Quantification of septum types in Erg25 OE (n=484), *scs22* $\Delta$  (n=391), *scs22* $\Delta$  Erg25 OE (n=469), *scs2* $\Delta$  cells (n=308), *scs2* $\Delta$  Erg25 OE (n=336), *scs22* $\Delta$ *scs2* $\Delta$  (n=413) and *scs22* $\Delta$ *scs2* $\Delta$  Erg25 OE cells (n=377). Error bars: SD.

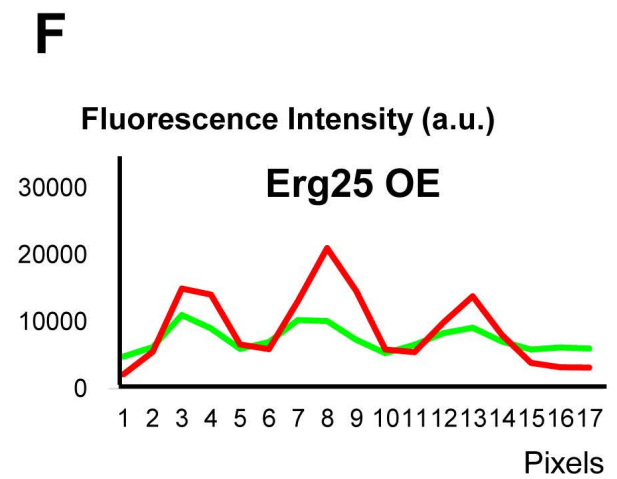
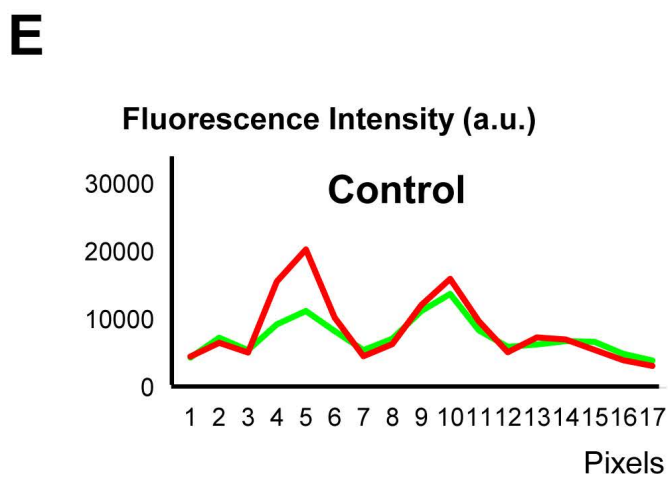
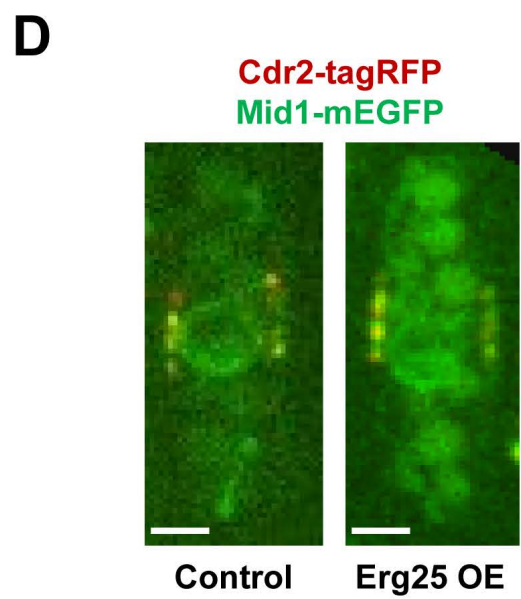
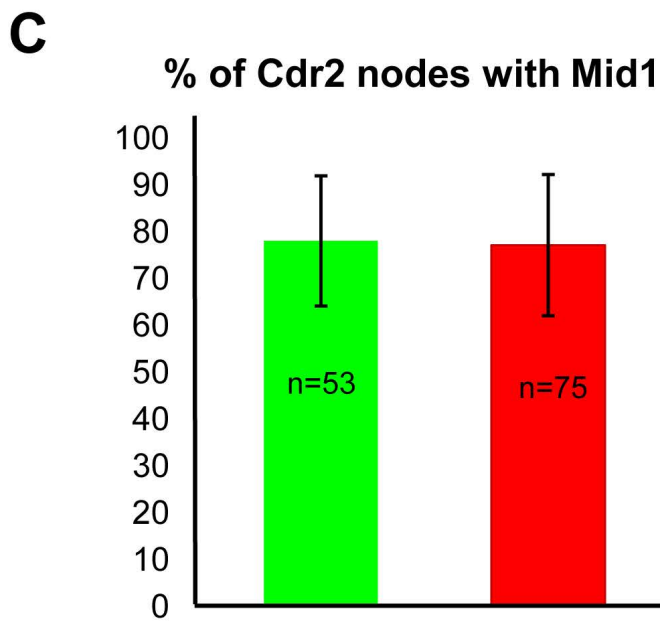
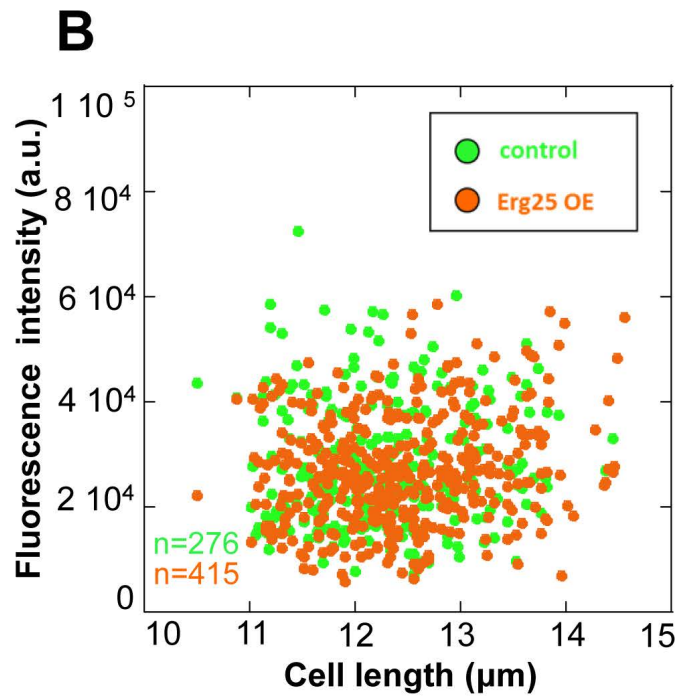
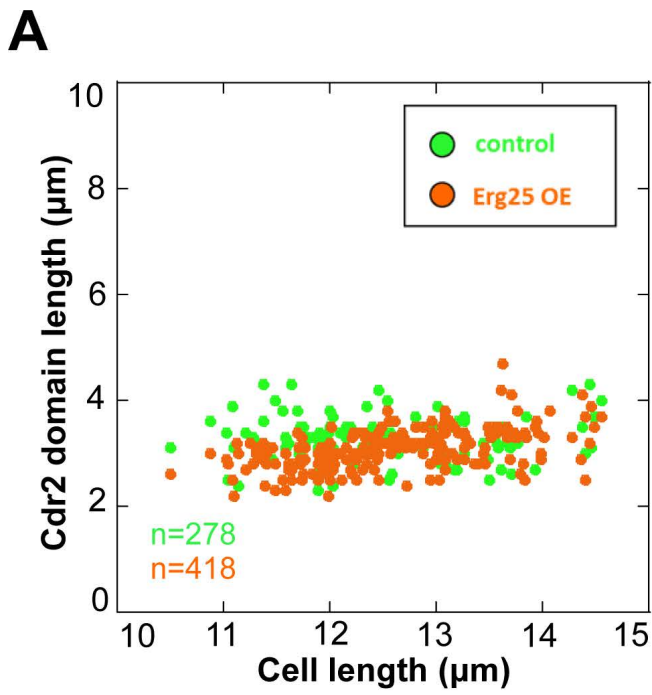




**Figure S2. Characterization of Cdr2 and Mid1 domains upon Erg25OE.**

**A:** Length of the Cdr2-EGFP domain relative to cell length in control (n=278) and Erg25 OE cells (n=418). **B:** Integrated fluorescence intensity (a.u.) of Cdr2-EGFP domain relative to cell length in control (n=278) and Erg25 OE cells (n=418). **C:** Percentage of Cdr2-tagRFP nodes containing Mid1-mEGFP in single cells. Error bars: SD (n>50 cells, top right). **D:** Medial planes confocal images of Mid1-mEGFP and Cdr2-tagRFP in control (left) and Erg25 OE cells (right). Scale bar, 5  $\mu$ m. **E-F:** Linescan analyzing Mid1-mEGFP and Cdr2-tagRFP intensity along the medial cortex (bottom) along the cells shown at the top right.



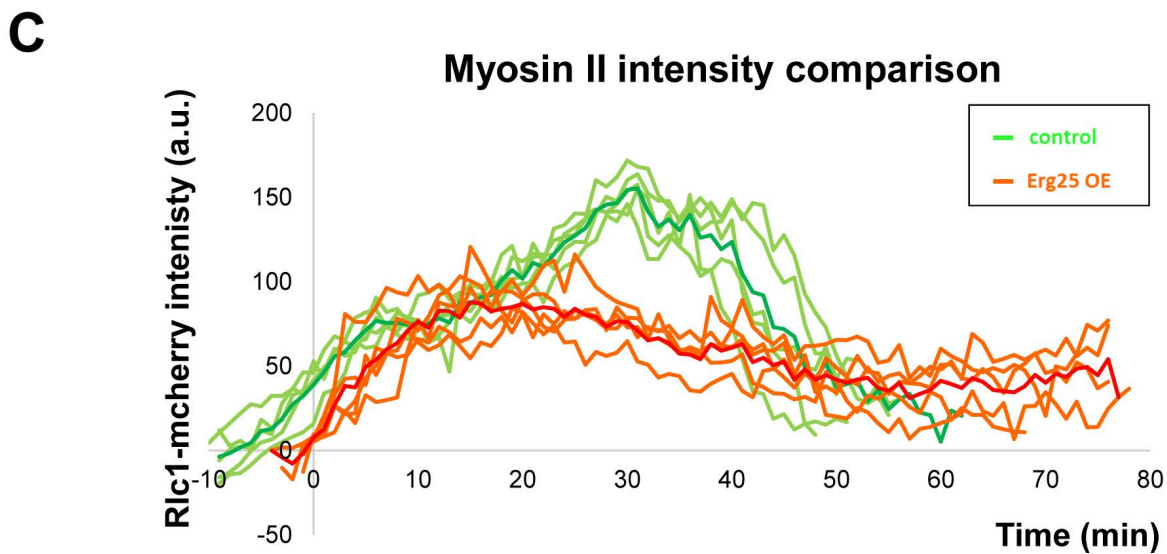
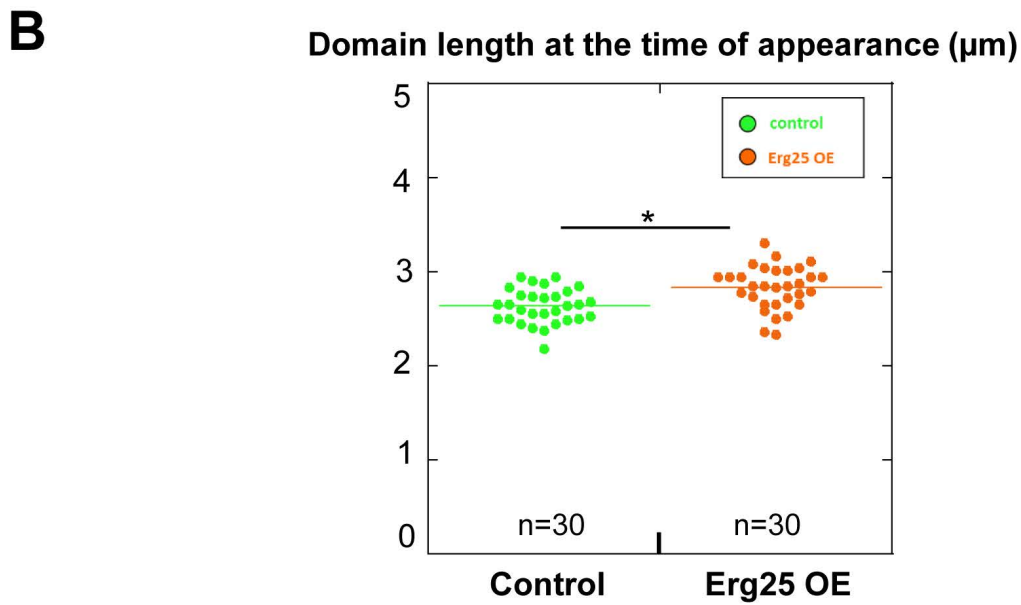
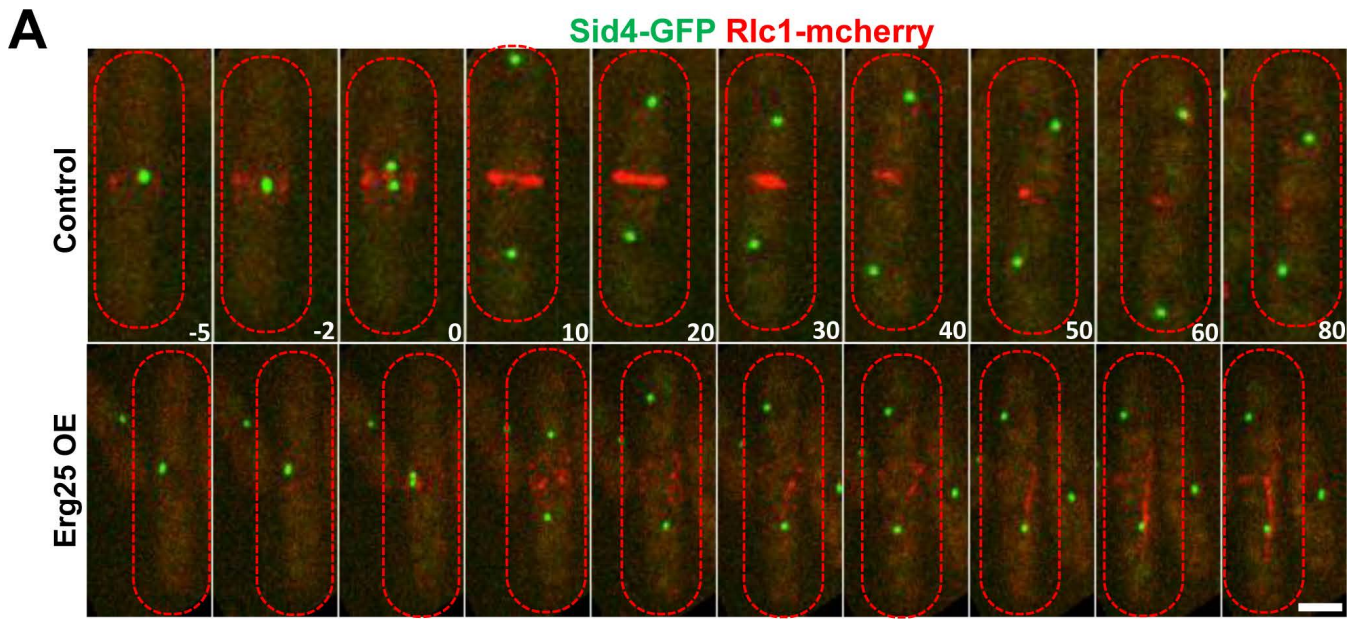


**Figure S3. Analysis of myosin II behavior in Erg25 OE cells.**

**A:** Time-lapse analysis of Sid4-GFP and Rlc1-mcherry in control (top) and Erg25 OE cells (bottom). Medial plane confocal images are shown. Time 0 corresponds to mitotic entry. Scale bars: 5  $\mu$ m. **B:** Measurement of myosin II domain length at the time of its initial recruitment in control and Erg25 OE cells (n=30). **C:** Analysis of myosin II intensity (a.u.) in the central region in control and Erg25 OE cells (n=5). t=0 corresponds to SPB separation.

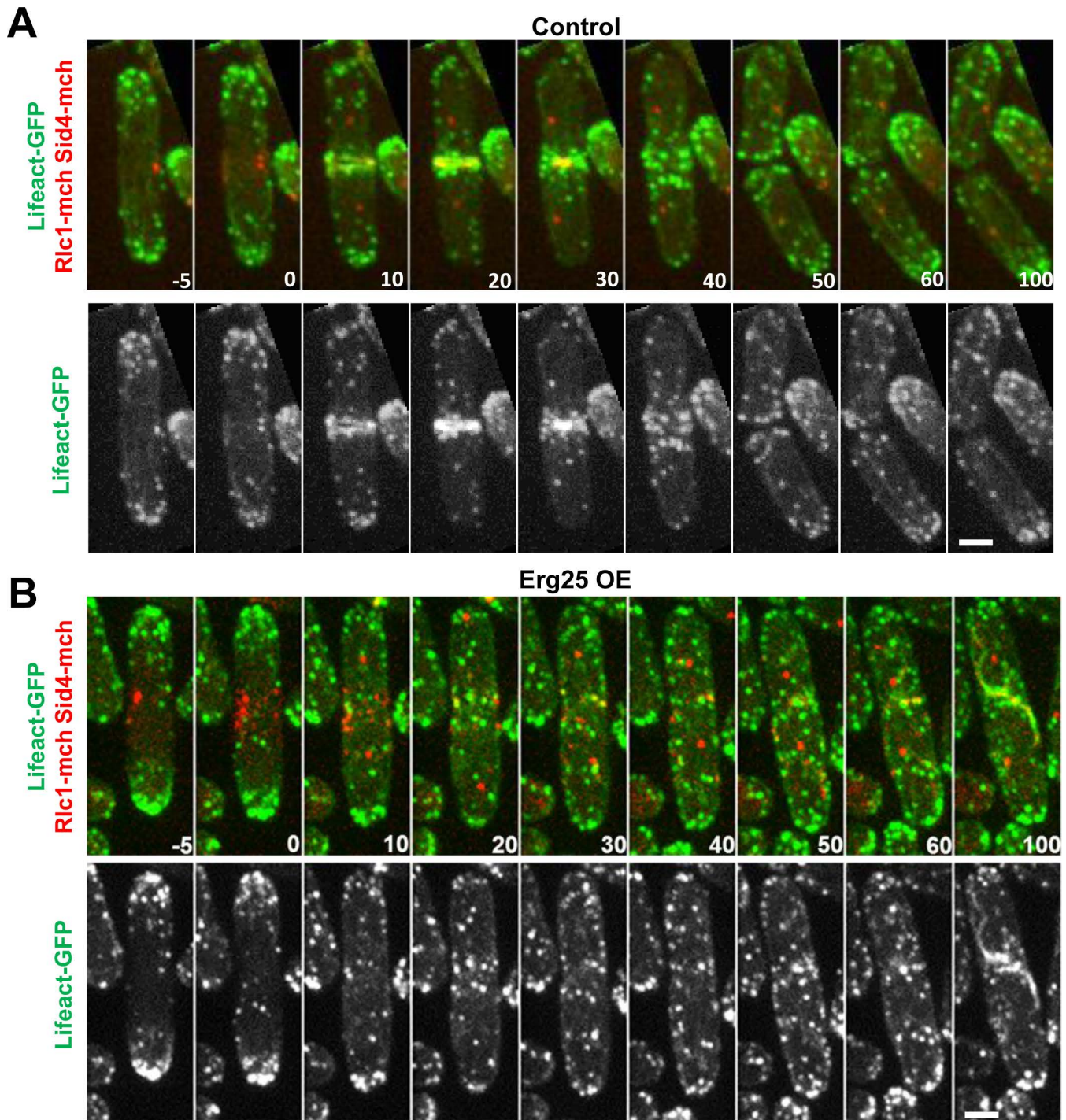


**Figure S4: Inhibition of F-actin nucleation from cytokinetic precursor nodes upon Erg25 OE**

Time-lapse images of control (A) and Erg25 OE cells (B) expressing lifeact-GFP, Rlc1-mcherry and Sid4-mcherry. Time 0 corresponds to mitotic entry. Scale bars: 5µm.



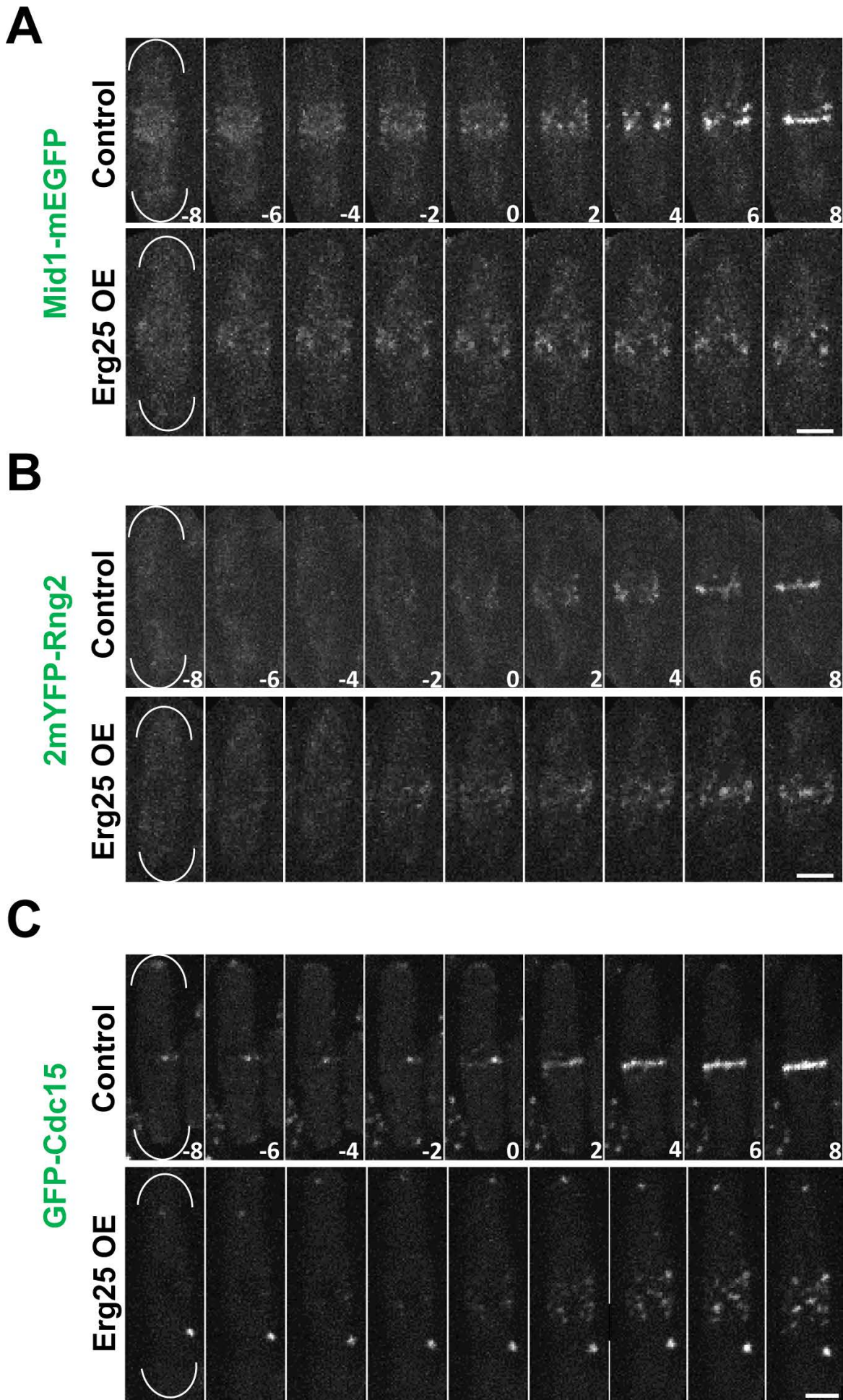


**Figure S5. Analysis of Mid1, Rng2 and Cdc15 by time lapse imaging upon Erg25 OE.**

Time lapse images of Mid1-mEGFP (**A**), 2mYFP-Rng2 (**B**) and GFP-Cdc15 (**C**) in control (top) and Erg25 OE cells (bottom). Time 0 corresponds to the time of SPB separation. Scale bar, 5  $\mu$ m.

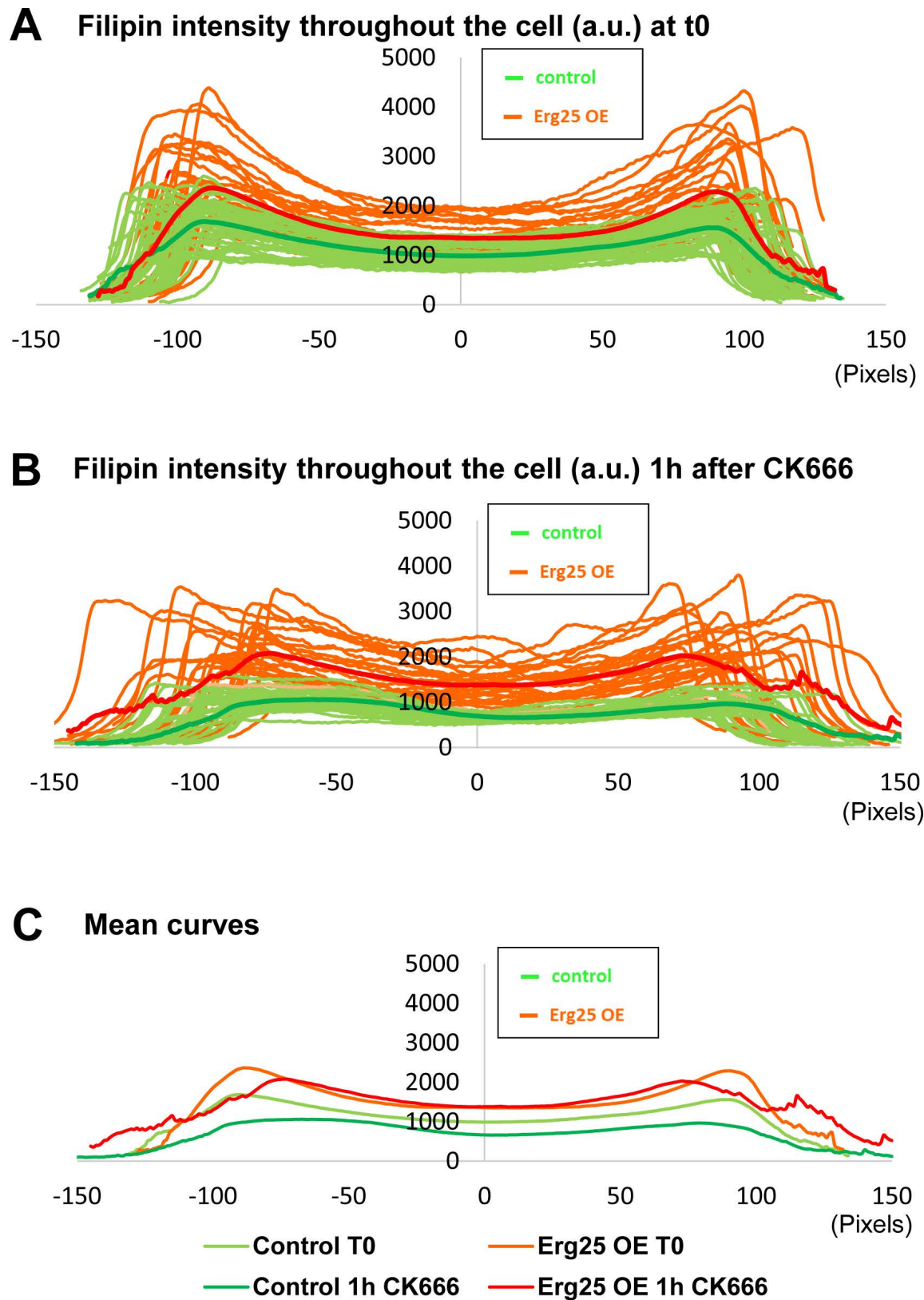
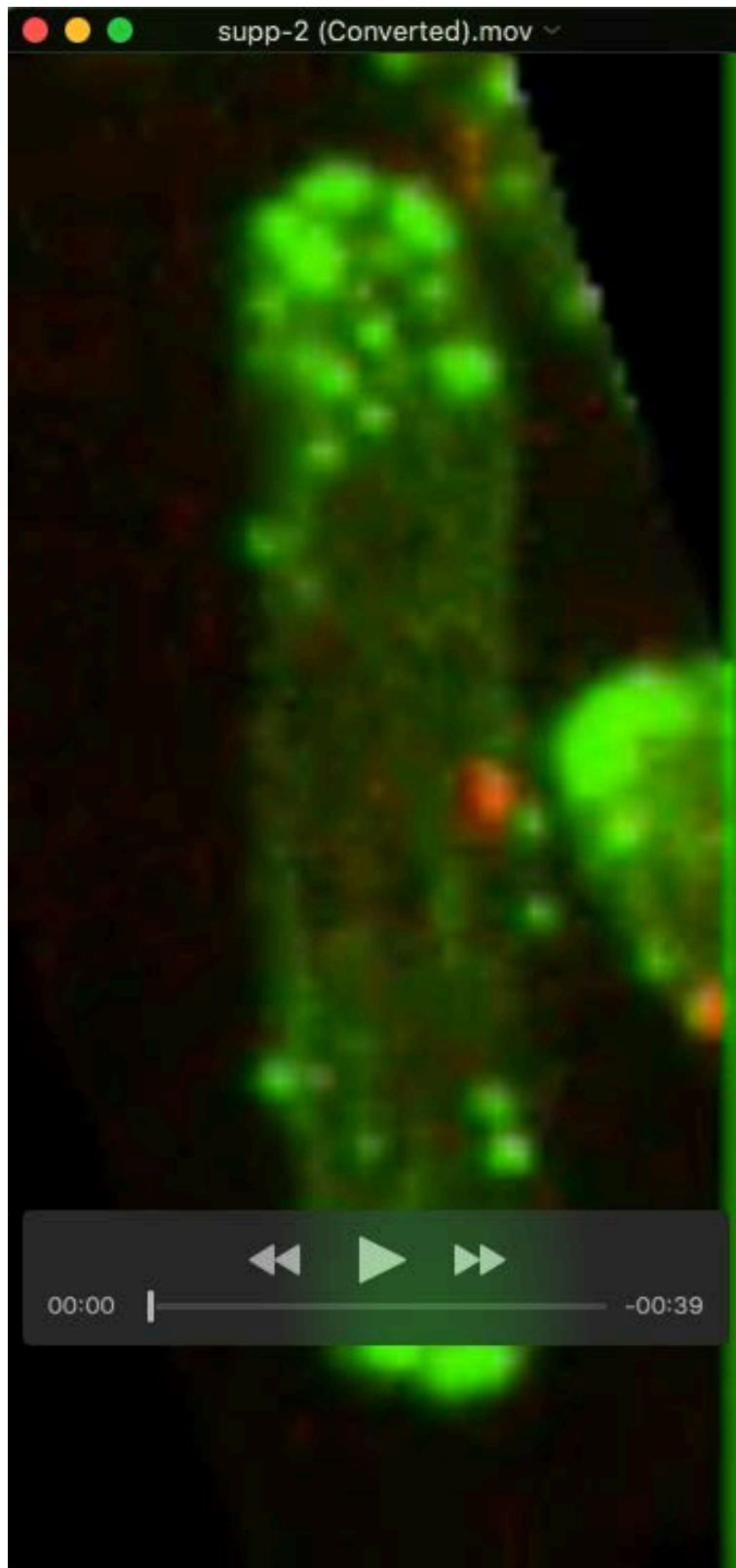


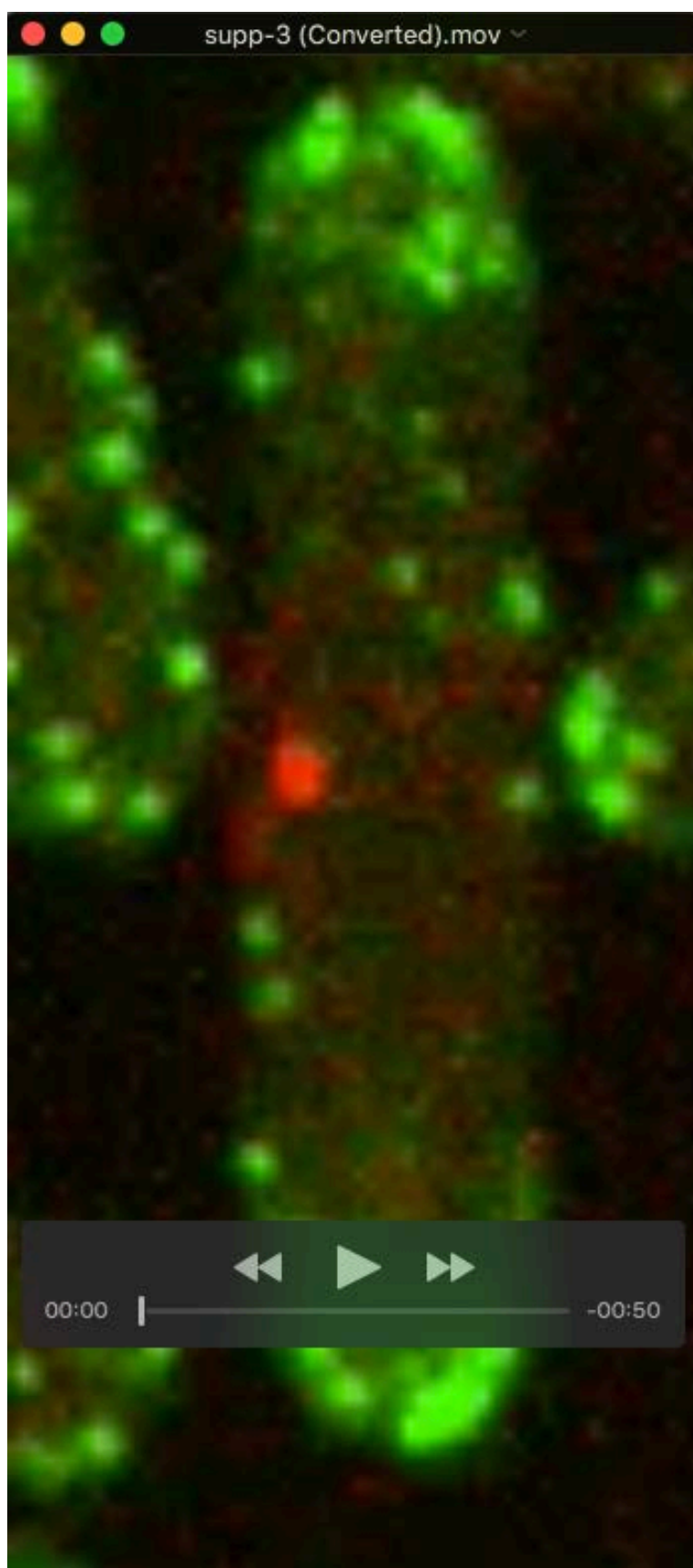
**Figure S6. Measurement of Ergosterol levels after treatment with CK666**

**A-B:** Filipin intensity expressed in a.u. was measured in control and Erg25 OE cells at time 0 (**A**) and after 1h of CK666 treatment (n=30 cells) (**B**). **C:** Graph showing the average curves of filipin intensity of control and Erg25 OE cells at time 0 and after 1h treatment with CK666.



**Movie 1.** F-actin dynamic distribution in a representative dividing control cell.





**Movie 2.** F-actin abnormal organization upon Erg25 OE.



**Movie 3.** Multiple examples of F-actin aberrant organization upon Erg25 OE in comparison with control cells.